



# Innovative spectral investigations on the thermal-induced poly(aspartic acid)

Bingjie Sun, Weizhen Li, Peiyi Wu\*

The Key Laboratory of Molecular Engineering of Polymers, Ministry of Education, Department of Macromolecular Science and Advanced Materials Laboratory, Fudan University, Handan Road 220, Shanghai 200433, PR China

## ARTICLE INFO

### Article history:

Received 12 January 2008

Received in revised form 12 April 2008

Accepted 17 April 2008

Available online 20 April 2008

### Keywords:

Poly(aspartic acid)

FTIR

2D correlation spectroscopy

## ABSTRACT

Two-dimensional (2D) correlation FTIR spectroscopy was used to investigate the dynamic mechanism of poly(aspartic acid) during the heating process. According to the 2D asynchronous correlation spectra, the C=O vibration band of Amide I was separated into three peaks at 1637, 1645 and 1677  $\text{cm}^{-1}$ , assigned to  $\alpha$  helical, random coil and  $\beta$  antiparallel conformation, respectively. And  $\alpha$  helical structure would transform into the more ordered and stable conformation of  $\beta$  antiparallel in heating. In the region of 3700–2700  $\text{cm}^{-1}$ , the H-contained groups were analyzed; the loosening of hydroxyl is found to change prior to the NH-related hydrogen bonds and the conformational reorganization of hydrocarbon chains.

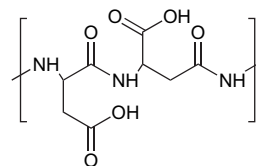
© 2008 Elsevier Ltd. All rights reserved.

## 1. Introduction

During the last several decades, the potential environmental damages caused by uncontrolled release and accumulation of the synthetic water-soluble polymers have involved more attentions. Poly(amino acids) with protein-like amide linkages may greatly improve this problem; they offer fully biodegradable polymers desirable for many applications. Poly(aspartic acid) (PASP hereafter) is one of this poly(amino acid) with acid side groups; its chemical structure is shown in Scheme 1. PASP can be synthesized either by hydrolysis of polysuccinimide (PSI) or by thermal polymerization of aspartic acid monomer with or without catalyst [1–3]. Low-cost manufacturing processes have been developed to synthesize PASP for commercial use as well. It is a promising developmental material with many advantages, such as nontoxic, water-solubility and biodegradable, these properties will have lots of potential uses, especially in biomedical and industrial applications. As biomedical materials [4,5], PASP is quite useful in sustained drugs' release, enzyme carriers, drug antigenicity blockers, artificial skin, wound covering materials and cell culture carriers. PASP has also been widely used in the industry as the detergent additive (polycarboxylic sequestrant), the dispersant to prevent the redeposition of minerals, the inhibitor of the salt crystallization and precipitation, or the water softener and corrosion inhibitor [6–10]. Early works [3,11] show that PASP hydrolyzed from PSI is composed of  $\alpha$  and  $\beta$  aspartic residues derived from different ring-opening mechanisms. By  $^1\text{H}$  NMR experiments, it was found that  $\alpha$  and

$\beta$  copolymer units were distributed in the main chain with a composition ratio of 25%  $\alpha$  and 75%  $\beta$  units [3].  $\alpha$  subunit is a standard protein unit, and Lagant et al. [12] have reported that the change of pH values can affect the formation of  $\alpha$  helical and  $\beta$  antiparallel structures in poly(aspartic acid).

The basic concept of constructing two-dimensional (2D) correlation spectroscopy was first introduced by Noda [13]. Using a generally applicable mathematical formalism, the generalized 2D correlation spectroscopy allows one to construct 2D correlation spectra from variations of spectra having an arbitrary waveform [14]. This generalized 2D correlation spectroscopy was found to be applicable to intensity fluctuations not only in time but also in any other physical or chemical disturbing variable, such as temperature [15–17], time [18], pressure [19,20], electric field strength [21,22], or concentration [23,24]. Subtle information not obvious in 1D spectra can be captured by 2D spectra due to spreading the peaks over the second dimension and improving the resolution of the spectra [25–28], and it is especially powerful in analyzing broad and overlapped bands like Amides I and II region. Therefore, 2D correlation FTIR spectroscopy has been extensively used to investigate the secondary structures, denaturalization, folding, and hydration process of proteins. Additionally, 2D correlation spectra



Scheme 1. Chemical structure of poly(aspartic acid).

\* Corresponding author. Fax: +86 21 65640293.

E-mail address: [peiyiwu@fudan.edu.cn](mailto:peiyiwu@fudan.edu.cn) (P. Wu).

can also provide the useful information about specific event sequence of different molecular segments in the perturbing process.

In this work the microgroups like carbonyl and hydrogen-bonded NH groups in the amide structures of PASP were investigated by FTIR spectroscopy. And 2D-IR correlation spectroscopy served as an innovative and useful technique to analyze the temperature-induced dynamic mechanism of PASP.

## 2. Experimental

### 2.1. Sample preparation

Thermal polymerization method of dry L-aspartic acid was used to synthesize polysuccinimide (PSI). Typically, L-aspartic acid (30.0 g/mol) and phosphoric acid (85%, 3.3 g) were charged into a three-necked round bottom flask and stirred under reduced pressure at 200 °C for 2 h. Then the reaction mixture was cooled and dissolved in DMF. The solution was precipitate in excess water and the precipitate was washed with water to remove the phosphoric acid. The final PSI product was dried at 80 °C under vacuum for 24 h. Two grams of PSI was dissolved in 10 ml deionized water, and was stirred for 10 min at room temperature to obtain molecularly dispersed and homogeneous solution. Then 0.825 g NaOH in 2 ml of deionized water was added dropwise at 0 °C to the solution. The solution was stirred for 3 h at room temperature, an appropriate amount of 0.1 M HCl was added until pH of the solution was 5, and was then dialyzed against deionized water for 48 h. The white powder of PASP was obtained after freeze-drying.

The molecular weight of PASP,  $M_w = 1.0 \times 10^4$  was determined by gel permeation chromatography. [HP series 1100 Chromatograph, Zorbax columns and RI/UV dual-mode detectors. The elution rate of 0.1 M NaNO<sub>3</sub> is 0.5 ml/min and standard PEG was used as calibration.] The composition ratio of the  $\langle\alpha\rangle$  and  $\langle\beta\rangle$  units is about 1:3 according to the <sup>1</sup>H NMR results. [<sup>1</sup>H NMR analysis was carried out on Philips DMX500 Spectrometer with DMSO-d<sub>6</sub> as the solvent.]

### 2.2. Fourier transform infrared spectroscopy

PASP was blended to a 1% concentration with KBr and pressed into a disk. This disk was sandwiched between two KBr windows and transferred to a temperature cell in the spectrometer. The FTIR measurements were performed at a resolution of 4 cm<sup>-1</sup> with a Nicolet 470 FTIR spectrometer equipped with a DTGS detector. Spectra were recorded in a temperature variable cell between 30 and 100 °C with intervals of 10 °C. The spectra used for the analysis were obtained from the subtraction of the background and the sample spectra at varying temperatures.

### 2.3. The 2D correlation analysis

Several spectra with equal temperature intervals were selected for the 2D correlation analysis using Matlab software. The average 1D spectrum was calculated as the reference spectrum and shown at the side and top of the 2D correlation maps. In the 2D correlation maps, unshaded regions indicate positive correlation intensities, while shaded regions indicate negative correlation intensities.

## 3. Results and discussion

### 3.1. FTIR analysis

Fig. 1 shows temperature-induced spectral changes of PASP sample from 30 to 100 °C. In the IR spectroscopy, there are two important regions for the analysis of poly(amino acids). One is the

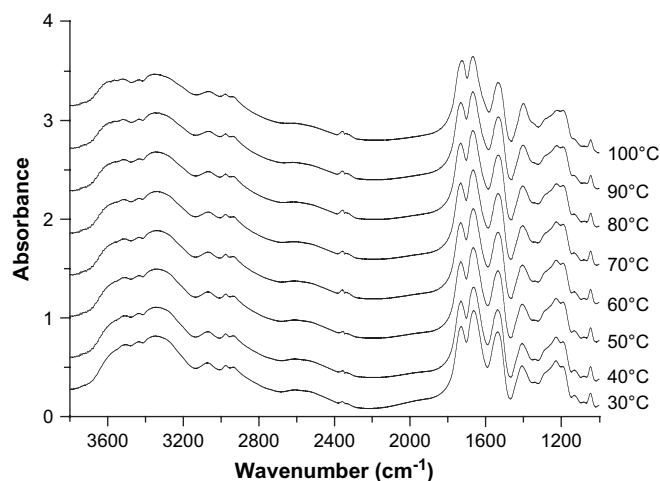


Fig. 1. Temperature-dependent IR spectra of PASP from 30 to 100 °C.

region of 1900–1460 cm<sup>-1</sup>, which is associated with the Amide I bands mainly induced by C=O stretching vibration [12,25,29,30] and the other one is the region of 3800–2700 cm<sup>-1</sup>, which contains the vibrational bands of the OH, NH and CH groups [31,32]. For convenient analysis, the IR spectra are divided into these two important parts in further discussions.

Fig. 2 shows the temperature-dependent IR spectra of PASP in 1900–1460 cm<sup>-1</sup> from 30 to 100 °C. Some changes in the intensities of the bands can be observed in the spectra, the band of  $\nu(\text{C}=\text{O})$  in amide groups at around 1645 cm<sup>-1</sup> decreased, but the intensity of the band of  $\nu(\text{C}=\text{O})$  in carboxylic group at around 1731 cm<sup>-1</sup> increased oppositely with the rising temperature [12,25,29]. More details will be explained in 2D-IR analysis below.

The IR spectra of PASP in the region of 3800–2700 cm<sup>-1</sup> during heating are shown in Fig. 3, the temperature-induced changes of  $\nu(\text{NH})$  bands can be seen in it. Two bands at around 3000–2700 cm<sup>-1</sup> are attributed to the  $\nu(\text{C}-\text{H})$  stretching modes [32]. Wu and Siesler has assigned the small band at 3066 cm<sup>-1</sup> to the first overtone of the Amide II mode at about 1533 cm<sup>-1</sup>, and the band at 3339 cm<sup>-1</sup> is assigned to the stretching mode of the hydrogen-bonded NH species  $\nu(\text{NH})_b$  [32]. As the band of  $\nu(\text{OH})$  stretching vibration at around 3500–3400 cm<sup>-1</sup> is too strong the band of free NH species  $\nu(\text{NH})_f$  is overlapped with it and cannot be seen in these spectra. From this figure, we can clearly observe that all the bands in the region of 3800–2700 cm<sup>-1</sup> decreased as the temperature increased.

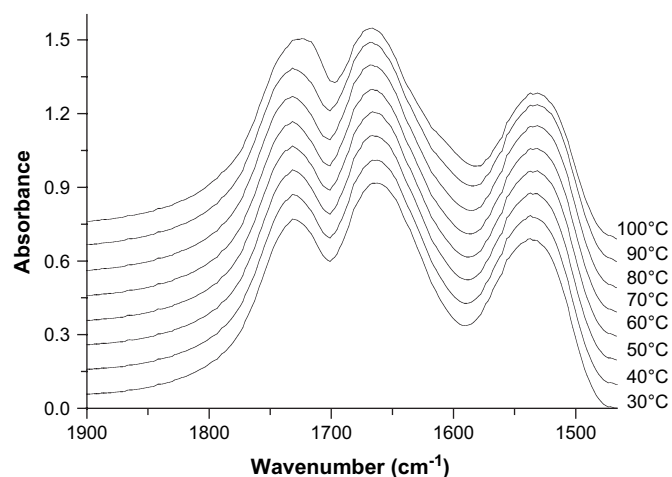


Fig. 2. Temperature-dependent IR spectra of PASP in the range of 1900–1460 cm<sup>-1</sup> from 30 to 100 °C.

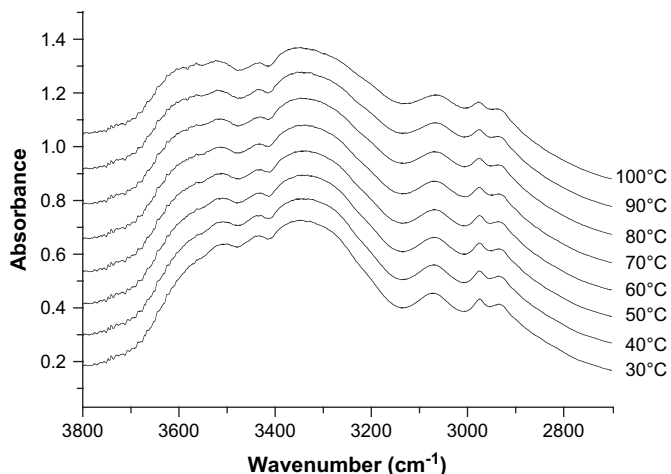


Fig. 3. Temperature-dependent IR spectra of PASP in the range of 3800–2700  $\text{cm}^{-1}$  from 30 to 100  $^{\circ}\text{C}$ .

### 3.2. The 2D correlation analysis

The 2D-IR correlation spectra have two independent wavenumber axes ( $\nu_1$ ,  $\nu_2$ ), which correlate with an intensity axis. There are two types of spectra in general, 2D synchronous and asynchronous. The 2D synchronous correlation spectrum is symmetric with respect to the diagonal line in it. The correlation intensity in the 2D synchronous maps reflects the relative degree of in-phase response. The peaks appearing along the diagonal are called autopeaks, which are always positive. Autopeaks reflect the peaks with great change under environmental perturbation. The off-diagonal peaks in the synchronous map are named crosspeaks, the symbols of them can be either positive or negative. Positive synchronous crosspeaks indicate that the intensity variations at wavenumber  $\nu_1$  and  $\nu_2$  proceed in the same direction upon perturbation, while negative crosspeaks show the changes are in opposite direction, i.e. the intensity of one band is increasing but that of the other band is decreasing.

The 2D asynchronous correlation spectrum is asymmetric with respect to the diagonal line. However, there is no autopeak within the asynchronous map; the only peaks appear are the off-diagonal crosspeaks, which can be either positive or negative. The intensities of the crosspeaks in the asynchronous spectrum represent the relative degree of out-of phase response of the peaks.

The crosspeaks appearing in both synchronous and asynchronous correlation spectra can help to obtain the specific sequences of the spectral intensity changes taking place under some environmental perturbations. According to Noda's rule [33], when the symbols of the crosspeak in the synchronous and asynchronous maps are the same (both positive or negative), peak  $\nu_1$  will change before peak  $\nu_2$  under the perturbation, but if the symbols of the crosspeak in the synchronous and asynchronous correlation spectroscopies are different (one is positive and the other one is negative), peak  $\nu_2$  will vary prior to  $\nu_1$ .

#### 3.2.1. The 2D analysis in the range of 1900–1600 $\text{cm}^{-1}$

Fig. 4(a) shows the synchronous 2D-IR spectrum of PASP in the range of 1900–1600  $\text{cm}^{-1}$  during heating. There are two strong autopeaks at 1712 and 1645  $\text{cm}^{-1}$  corresponding to the vibration of  $\nu(\text{C}=\text{O})$  in carboxylic groups and Amide I, respectively [12,25,29]. The crosspeak between them at 1712 and 1645  $\text{cm}^{-1}$  is negative, which indicates that the heat-induced intensity variations of these two peaks at 1712 and 1645  $\text{cm}^{-1}$  take place in opposite directions. This result is in accordance with the 1D-IR spectra of Fig. 2 that the peak intensity of  $\nu(\text{C}=\text{O})$  in carboxylic groups increases but that of  $\nu(\text{C}=\text{O})$  in amide groups decreases with the rising temperature.

Fig. 4(b) shows the 2D asynchronous spectrum of PASP in 1900–1600  $\text{cm}^{-1}$  as temperature rises. Three negative crosspeaks: A(1677, 1637), C(1756, 1645), E(1712, 1689)  $\text{cm}^{-1}$ , and two positive crosspeaks: B(1756, 1712), D(1712, 1637)  $\text{cm}^{-1}$ , are obtained in this map. The existence of crosspeak A(1677, 1637)  $\text{cm}^{-1}$  clearly indicates that the Amide I band was split into two separate peaks at 1677 and 1637  $\text{cm}^{-1}$  (these peaks were overlapped with each other in the 1D-IR spectra). The peak at 1637  $\text{cm}^{-1}$  is assignable to  $\alpha$  helical conformation, while that at 1677  $\text{cm}^{-1}$  is due to  $\beta$  antiparallel conformation, and their assignments are listed in Table 1 [12,25,29]. The crosspeak A(1677, 1637)  $\text{cm}^{-1}$  can be observed to be positive in Fig. 4(a), as the symbols of crosspeak A(1677, 1637)  $\text{cm}^{-1}$  in the 2D maps are different (in the synchronous map positive, in the asynchronous map negative), according to Noda's rule [33], we can conclude that the temperature-induced variations of the spectral intensity at 1637  $\text{cm}^{-1}$  occur earlier than 1677  $\text{cm}^{-1}$ , which means  $\alpha$  helical conformation is more sensitive to heat than  $\beta$  antiparallel conformation. As  $\beta$  antiparallel structure is more ordered and stable, it can be hypothesized that part of  $\alpha$  helical conformation tends to transfer to  $\beta$  antiparallel conformation during heating, therefore the  $\alpha$  helical conformation will change first as long as the temperature of the system is raised.

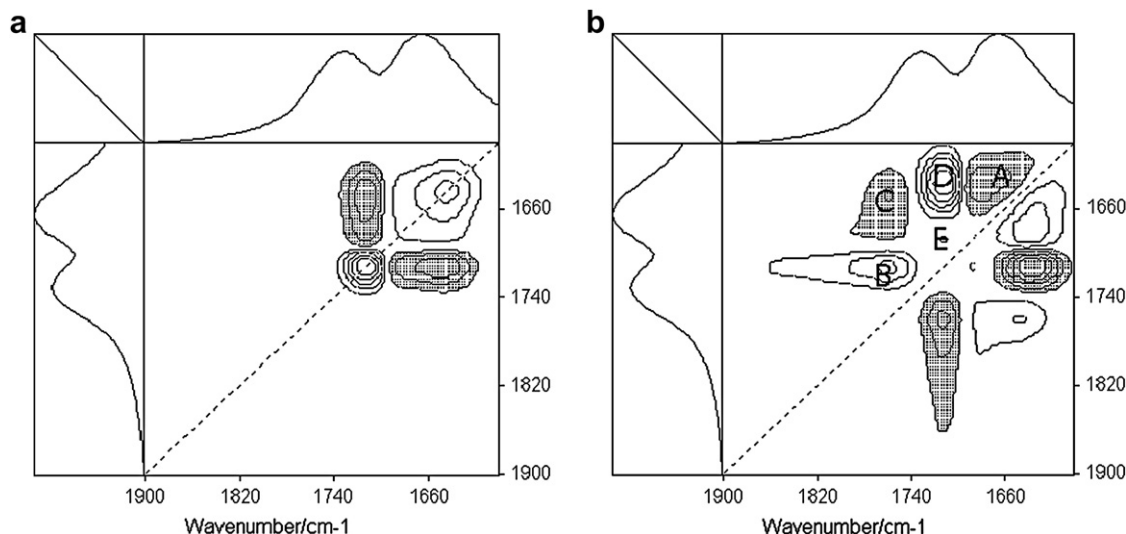


Fig. 4. Synchronous (a) and asynchronous (b) 2D FTIR spectrum of PASP in the range of 1900–1600  $\text{cm}^{-1}$  from 30 to 100  $^{\circ}\text{C}$ .

**Table 1**

Wavenumbers ( $\text{cm}^{-1}$ ) and assignments of IR bands for PASP in the range of 1900–1600  $\text{cm}^{-1}$  [12,25,29]

Wavenumber ( $\text{cm}^{-1}$ )	Assignments
1756	Free COOH group
1712	Weak-hydrogen-bonded COOH group
1689	Strong-hydrogen-bonded COOH group
1677	$\beta$ Antiparallel
1645	Random coil
1637	$\alpha$ Helical

The appearance of crosspeaks at B(1756, 1712) and E(1712, 1689)  $\text{cm}^{-1}$  shows that the band at 1731  $\text{cm}^{-1}$  in 1D-IR spectra was split into three separate peaks at 1756, 1712 and 1689  $\text{cm}^{-1}$ , which were assigned to the vibration of  $\nu(\text{C}=\text{O})$  in free COOH groups, weak-hydrogen-bonded COOH groups and strong-hydrogen-bonded COOH groups, respectively [25,29]. It has been known that crosspeak B(1756, 1712) is positive and E(1712, 1689)  $\text{cm}^{-1}$  is negative in the asynchronous map, with the help of the slice spectra (not show), both B and E are found to be negative in the synchronous map of Fig. 4(a). Therefore, according to Noda's rule [33], the changing sequence of these peaks can be obtained as: 1712 > 1756 and 1689  $\text{cm}^{-1}$ , which means that the weak-hydrogen-bonded COOH groups varied prior to the free COOH groups and the strong-hydrogen-bonded COOH groups during heating.

In the slice spectra of Fig. 4(a), the crosspeaks at C(1756, 1645) and D(1712, 1637)  $\text{cm}^{-1}$  are also found to be negative, which help to infer that 1637 > 1712  $\text{cm}^{-1}$ ; 1756 > 1645  $\text{cm}^{-1}$ . With their assignments in Table 1, we can conclude that during heating  $\alpha$  helical configuration changed prior to the transformation among free and hydrogen-bonded COOH groups and free COOH groups changed prior to the random coil structures.

### 3.2.2. The 2D analysis in the range of 3700–2700 $\text{cm}^{-1}$

Fig. 5(a) shows the synchronous 2D-IR spectrum of PASP in the range 3700–2700  $\text{cm}^{-1}$  during heating. The relationships between variations of the H-contained vibrations like  $\nu(\text{OH})$ ,  $\nu(\text{NH})$  and  $\nu(\text{CH})$  will be focused on within this region. The assignments of these bands are summarized in Table 2 [31,32]. The synchronous map in Fig. 5(a) is rather featureless, except the domination of a broad autopeak encompassing the entire region. This phenomenon indicates that the overall spectral intensities in this region change towards the same direction with the rising temperature. According to the results of Fig. 3, we can deduce that all the bands decreased.

**Table 2**

Wavenumbers ( $\text{cm}^{-1}$ ) and assignments of IR bands for PASP in the range of 3700–2700  $\text{cm}^{-1}$  [31,32]

Wavenumber ( $\text{cm}^{-1}$ )	Assignments
3455, 3475	$\nu(\text{OH})$
3066	Overtone of Amide II (C–N and N–H)
3317, 3228	$\nu(\text{NH})$
2904, 2969	$\nu(\text{CH})$

More information can be obtained from the corresponding asynchronous spectrum of PASP in Fig. 5(b). In the asynchronous map, one negative crosspeak at (3317, 3228)  $\text{cm}^{-1}$  can be observed, which indicates that the band of  $\nu(\text{NH})_b$  at 3339  $\text{cm}^{-1}$  in 1D-IR spectrum was split into two components at 3317 and 3228  $\text{cm}^{-1}$ ; this split is due to the existence of different forms of NH-related hydrogen bonds (there should be a band assigned to the weakest NH hydrogen bond at higher wavenumber than 3339  $\text{cm}^{-1}$ , however, the change of this band is too small compared to the other two bands during the heating process, therefore it is difficult to find it in the above-mentioned 2D-IR spectrum, which can only reflect the bands with relatively large changes). The crosspeak at (3317, 3228)  $\text{cm}^{-1}$  is found to be positive in the synchronous map, therefore we can conclude with Noda's rule [33] that the variations of the spectral intensity at 3228  $\text{cm}^{-1}$  occur earlier than those at 3317  $\text{cm}^{-1}$ , this changing order may reflect the transformation effect between two species of NH-related hydrogen bonds during heating.

In the asynchronous map three other positive crosspeaks at (3455, 2904), (3455, 2969), and (3475, 3317)  $\text{cm}^{-1}$  can also be found. As their symbols in the corresponding synchronous map are all positive, we can infer the vibrations' changing sequence of PASP as 3455 > 2904, 2969 and 3475 > 3317  $\text{cm}^{-1}$ . With the assignments of these peaks in Table 2, we can understand that the vibrational changes of the OH groups were prior to both the CH and the NH groups. To further ascertain the changing order between the latter two groups, we made the slice spectrum of the asynchronous map (not show) and observed the positive crosspeak of (3317, 2904)  $\text{cm}^{-1}$ , as it is also positive in the synchronous map, we can infer 3317 > 2904  $\text{cm}^{-1}$ , which means that the vibration of the NH groups changed earlier than the CH groups. To sum up with all the changing sequences gained above, the whole dynamic order of the PSAP sample can be received as  $\nu(\text{OH}) > \nu(\text{NH}) > \nu(\text{CH})$ . This result reveals that the conformational changes of the hydroxyl group proceed faster than those of the NH group and the slowest is

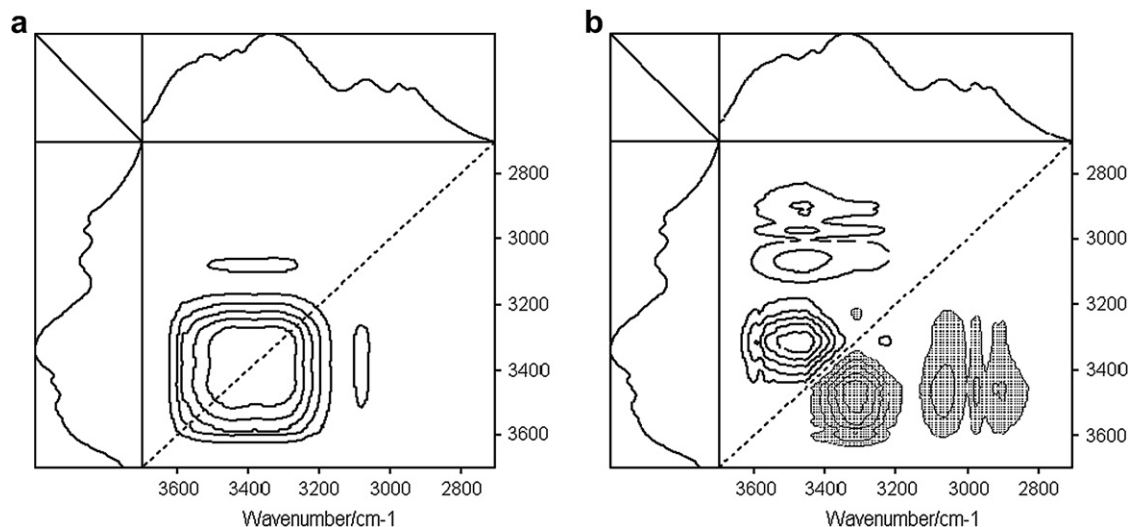


**Fig. 5.** Synchronous (a) and asynchronous (b) 2D FTIR spectrum of PASP in the range of 3700–2700  $\text{cm}^{-1}$  from 30 to 100 °C.

hydrocarbon chains, or, in other words, the hydrogen bonds become weaker before the hydrocarbon chains reorganize. This is quite consistent with the conclusion we gained in the PNIPAM dry films [31]. However, according to Wu's experience [32], the sequence of the spectral changes of NH and CH fundamental vibrations in temperature-induced polyamide 11 is opposite. It can be hypothesized that hydrocarbon chains of PASP are shorter than those of polyamide 11, or, which can be said to be more rigid and harder to reorganize, so the dissociation of hydrogen bonds of hydroxyl and NH groups precedes the conformational changes of the hydrocarbon chains. Chemical groups existing in different kinds of polymers may own various properties.

Furthermore the sequence of  $\nu(\text{OH}) > \nu(\text{NH})$  is raised by the secondary structure of amide acid. The secondary structure like  $\alpha$  helical and  $\beta$  antiparallel is built by N–H and C=O groups and the hydrogen bonds between them. The breakage of the hydrogen bonds formed by OH within side-chain COOH groups is prior to the destruction of hydrogen bonds of N–H $\cdots$ O=C in the secondary structure during heating.

#### 4. Conclusion

The 2D correlation FTIR spectroscopy was used to investigate the temperature-induced changes of chemical groups in poly(-aspartic acid).

1. In the range of Amide I at 1900–1460  $\text{cm}^{-1}$  C=O vibration bands were separated into three bands at 1637, 1645 and 1677  $\text{cm}^{-1}$ , which are assigned to  $\alpha$  helical, random coil and  $\beta$  antiparallel conformation, respectively. Through 2D-IR correlation spectroscopy the sequential order of intensity changes can be obtained:  $\alpha$  helical  $>$   $\beta$  antiparallel. It can be hypothesized that part of  $\alpha$  helical conformation tends to transfer to  $\beta$  antiparallel conformation during heating, as the structure of  $\beta$  antiparallel is more ordered and stable.
2. The sequence of the spectral changes of  $\nu(\text{OH})$ ,  $\nu(\text{NH})$ , and  $\nu(\text{CH})$  was inferred from the 2D-IR maps in the range of 3700–2700  $\text{cm}^{-1}$  as  $\nu(\text{OH}) > \nu(\text{NH}) > \nu(\text{CH})$ . The loosening of hydrogen bonds precedes the conformational reorganization of hydrocarbon chains. It can be hypothesized that hydrocarbon chains of PASP are shorter, or, which can be said to be more rigid and harder to reorganize, so the hydrogen bonds become weaker before the hydrocarbon chains reorganize during temperature increase. Additionally, the breakage of the hydrogen bonds formed by OH within side-chain COOH groups is earlier than the destruction of amide hydrogen bonds of N–H $\cdots$ O=C in the secondary structure during heating.

#### Acknowledgements

The authors gratefully acknowledge the financial support by the National Science of Foundation of China (NSFC) (Nos. 20774022, 20573022, 20425415, 20490220), the “Leading Scientist” Project of Shanghai (No. 07XD14002), the National Basic Research Program of China (2005CB623800) and Ph.D. Program of MOE (20050246010).

#### References

- [1] Katchalski E. *Advances in Protein Chemistry* 1951;6:123–85.
- [2] Tomida M, Nakato T, Matsunami S, Kakuchi T. *Polymer* 1997;38(18):4733–6.
- [3] Wolk SK, Swift G, Paik YH, Yocom KM, Smith RL, Simon ES. *Macromolecules* 1994;27(26):7613–20.
- [4] Giammona G, Giannola LI, Carlisi B, Bajardi ML. *Chemical and Pharmaceutical Bulletin* 1989;37(8):2245–7.
- [5] Willmott N, Chen Y, Florence AT. *Journal of Controlled Release* 1988;8(2):103–9.
- [6] Littlejohn F, Grant CS, Wong YL, Saez AE. *Industrial and Engineering Chemistry Research* 2002;41(18):4576–84.
- [7] Garris JP, Sikes CS. *Colloids and Surfaces A – Physicochemical and Engineering Aspects* 1993;80(2–3):103–12.
- [8] Mueller E, Sikes CS. *Calcified Tissue International* 1993;52(1):34–41.
- [9] Silverman DC, Kalota DJ, Stover FS. *Corrosion* 1995;51(11):818–25.
- [10] Littlejohn F, Saez AE, Grant CS. *Industrial and Engineering Chemistry Research* 1998;37(7):2691–700.
- [11] Pivcova H, Saudek V, Drobnik J, Vlasak J. *Biopolymers* 1981;20(8):1605–14.
- [12] Lagant P, Vergoten G, Loucheux C, Fleury G. *Polymer Journal* 1979;11(5):345–51.
- [13] Noda I. *Journal of the American Chemical Society* 1989;111(21):8116–8.
- [14] Noda I. *Applied Spectroscopy* 1993;47(9):1329–36.
- [15] Ozaki Y, Liu YL, Noda I. *Applied Spectroscopy* 1997;51(4):526–35.
- [16] Czarnicki MA, Maeda H, Ozaki Y, Suzuki M, Iwahashi M. *Applied Spectroscopy* 1998;52(7):994–1000.
- [17] Sun BJ, Lin YN, Wu PY, Siesler HW. *Macromolecules* 2008;41(4):1512–20.
- [18] Yu J, Wu PY. *Polymer* 2007;48(12):3477–85.
- [19] Magtoto NP, Sefara NL, Richardson HH. *Applied Spectroscopy* 1999;53(2):178–83.
- [20] Smeller L, Heremans K. *Vibrational Spectroscopy* 1999;19(2):375–8.
- [21] Ataka K, Osawa M. *Langmuir* 1998;14(4):951–9.
- [22] Gregoriou VG, Chao JL, Toriumi H, Palmer RA. *Chemical Physics Letters* 1991;179(5–6):491–6.
- [23] McClure WF, Maeda H, Dong J, Liu YL, Ozaki Y. *Applied Spectroscopy* 1996;50(4):467–75.
- [24] Sefara NL, Magtoto NP, Richardson HH. *Applied Spectroscopy* 1997;51(4):536–40.
- [25] Murayama K, Wu YQ, Czarnik-Matusewicz B, Ozaki Y. *Journal of Physical Chemistry B* 2001;105(20):4763–9.
- [26] Muller M, Buchet R, Fringeli UP. *Journal of Physical Chemistry* 1996;100(25):10810–25.
- [27] Wang Y, Murayama K, Myojo Y, Tsenkova R, Hayashi N, Ozaki Y. *Journal of Physical Chemistry B* 1998;102(34):6655–62.
- [28] Jung YM, Czarnik-Matusewicz B, Ozaki Y. *Journal of Physical Chemistry B* 2000;104(32):7812–7.
- [29] Nie BN, Stutzman J, Xie AH. *Biophysical Journal* 2005;88(4):2833–47.
- [30] Lu XL, Cheng I, Mi YL. *Polymer* 2007;48(3):682–6.
- [31] Sun BJ, Lin YN, Wu PY. *Applied Spectroscopy* 2007;61(7):765–71.
- [32] Wu P, Siesler HW. *Journal of Molecular Structure* 2000;521:37–47.
- [33] Noda I, Dowrey AE, Marcott C, Story GM, Ozaki Y. *Applied Spectroscopy* 2000;54(7):236a–48.